

# **Effect of Carbon on Primary Alpha Percentage in Ti-6Al-4V as Temperature Approaches the Beta Transus**

A Senior Project

presented to

the Faculty of the Materials Engineering Department

California Polytechnic State University, San Luis Obispo

In Partial Fulfillment

of the Requirements for the Degree

Bachelor of Science Materials Engineering

by

Kyle Savage

June, 2013

© 2013 Kyle Savage

## Approval Page

Project Title: Effect of Carbon on Primary Alpha Percentage in Ti-6Al-4V as Temperature Approaches the Beta Transus

Author: Kyle Savage

Date Submitted: June 7, 2013

CAL POLY STATE UNIVERSITY

Materials Engineering Department

Since this project is a result of a class assignment, it has been graded and accepted as fulfillment of the course requirements. Acceptance does not imply technical accuracy or reliability. Any use of the information in this report, including numerical data, is done at the risk of the user. These risks may include catastrophic failure of the device or infringement of patent or copyright laws. The students, faculty, and staff of Cal Poly State University, San Luis Obispo cannot be held liable for any misuse of the project.

Prof. Blair London

Faculty Advisor

\_\_\_\_\_

Signature

Prof. Richard Savage

Department Chair

\_\_\_\_\_

Signature

## Abstract

Some Ti-6Al-4V forgings require a specific amount of  $\alpha$  phase known as primary  $\alpha$  in the finished product. The percentage of primary  $\alpha$  is dependent on how close to the beta transus temperature forging is conducted. The beta transus temperature is affected by certain alloying elements. Carbon is one of the elements known to increase the beta transus temperature. Since each Ti-6Al-4V ingot contains varying amounts of carbon, testing on a variety of chemistries needs to be conducted. Cubes approximately 0.5 inches from low, medium, and high carbon chemistries were heat treated at temperatures below the beta transus in 18°F increments. Point counting was performed on metallographically prepared microstructures of each chemistry to find carbon's effect on primary  $\alpha$  percentage. The low and medium carbon samples showed linear trends with slopes of -0.249%  $\alpha$ /T and -0.276%  $\alpha$ /T respectively, and  $R^2$  values of 0.97 for both. The high carbon sample did not show the same linearity with an  $R^2=0.91$  for a linear regression, but had a slope of -0.392% $\alpha$ /T. Both the medium and high carbon compositions appeared to be shifted lower 5-10% primary  $\alpha$  percentage.

Keywords: titanium, primary alpha, Ti-6Al-4V, materials engineering, forging, beta transus

## **Acknowledgements**

Industrial Sponsor: Weber Metals Inc.

Industrial Contact: Arash Abadi

Advisor: Prof. Blair London

Additional thanks to Bob Hayes and MTI for cutting samples.

## Table of Contents

Abstract .....	2
Table of Contents .....	4
List of Figures .....	5
A. Introduction .....	6
A.1 Problem Statement .....	6
A.2 Titanium Background.....	6
A.3 Titanium Phases .....	8
A.3.1 Alpha Titanium .....	8
A.3.2 Beta Titanium .....	9
A.3.4 Beta to Alpha Transformation .....	9
A.4 Classifying Titanium Alloys .....	10
A.4.1 Alpha Alloys .....	11
A.4.2 Beta Alloys.....	12
A.4.3 Alpha-Beta Alloys.....	12
A.5 Ti-6Al-4V Microstructure .....	13
A.6 Titanium Forging.....	15
A.6.1 Primary Working.....	15
A.6.2 Die Forging .....	15
A.7 Broader Impacts .....	15
B. Experimental Procedure .....	16
B.1 Titanium Alloys .....	16
B.2 Sample Preparation .....	16
B.3 Testing Methodology.....	17
B.4 Realistic Constraints.....	21
C. Results.....	21
D. Discussion .....	26
E. Conclusions .....	27
F. References.....	28

## List of Figures

Figure 1. Tensile strength vs density for titanium and steel. Purple circles represent titanium alloys and teal represents steels. Light blue circles are specifically labeled titanium alloys and orange are specifically labeled steels <sup>2</sup> . ....	7
Figure 2. Specific strength vs temperature for titanium alloys and other structural materials <sup>1</sup> . ....	7
Figure 3. Hexagonal close packed structure of $\alpha$ -Ti with a) showing the lattice parameters and b) the slip planes <sup>1</sup> . ....	8
Figure 4. The $\beta$ to $\alpha$ transformation showing the (110) BCC planes in white and the (0001) HCP basal plane in gray <sup>1</sup> . ....	9
Figure 5. Body centered cubic structure of $\beta$ -Ti <sup>1</sup> . ....	9
Figure 6. Lamellar basket-weave structure of $\alpha$ -Ti in Ti-6Al-4V <sup>1</sup> . Alpha is the lighter color phase and beta is the darker color phase on the grain boundaries. ....	10
Figure 7. Schematic representation of the alloying element categories for titanium <sup>1</sup> . ....	10
Figure 8. Microstructures of Ti-6Al-4V under three cooling rates and at four temperatures <sup>5</sup> . For this project (b) is the expected microstructure when quenching from below and $\beta$ -transus, and (a) is the expected microstructure when quenching from above the $\beta$ -transus. ....	14
Figure 9. Diagram of locations on each converted ingot slice where cubes were cut. Both round (left) and square (right) slices were received.....	17
Figure 10. High temperature furnace and separate temperature readout used for heat treating. ....	17
Figure 11. Setup inside the furnace: blue arrows point to the furnace thermocouples, the green arrow points to the independent thermocouple, the red arrow points to the sample wrapped in steel wire, and the yellow arrows point to high temperature bricks. ....	18
Figure 12. Micrograph of a sample heat treated at 1735°F, quenched, then aged at 896°F. Overlaid is a 100 point grid representative of the grid used to point count. Circled in yellow is a primary $\alpha$ particle. .	20
Figure 13. Plots of average primary alpha percent for (a)the 0.012%C alloy, (b) the 0.020%C alloy, and (c) the 0.038%C alloy. Also shown are linear regression equations for each plot. The low and medium carbon alloys showed the most linearity.....	24
Figure 14. Boxplots for (a) the 0.012%C alloy, (b) the 0.020%C alloy, and (c) the 0.038%C alloy. The black represents the mean, the box represents the middle two quartiles of data, and the line through the box is the median. Outliers are shown by asterisks. The range was as large as 30% primary alpha for each sample, although most had a range of about 15% primary alpha. ....	25
Figure 15. Representative phase diagram for Ti-6Al-4V. Temperatures are only approximate. ....	26

## List of Tables

Table I.....	16
Table II.....	22

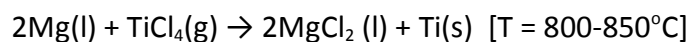
## A. Introduction

### A.1 Problem Statement

Ti-6Al-4V is an  $\alpha+\beta$  titanium alloy, which requires forging below the  $\beta$ -transus temperature; above the  $\beta$ -transus Ti-6Al-4V transforms into pure  $\beta$ , where uninhibited grain growth occurs due to the lack of a two phase microstructure. Carbon is known to increase the beta transus temperature, but a relationship between primary  $\alpha$  percent and carbon content is unknown. A relationship between carbon content and primary  $\alpha$  percent will be beneficial in predicting the percent  $\alpha$  of Ti-6Al-4V under forging conditions. Multiple compositions will be tested with varying carbon content to find a relationship between carbon content and primary  $\alpha$  percent as temperature approaches the  $\beta$ -transus.

### A.2 Titanium Background

Titanium oxide was discovered by British chemist William Gregor in 1791 by treating ilmenite with hydrochloric acid. In 1795 a chemist from Berlin, Martin Heinrich Klaproth, independently isolated titanium oxide from rutile, a mineral composed mainly of titanium dioxide. Klaproth named the new element “titanium” after the titans from Greek mythology. It was not until 1910 though that titanium itself was first isolated by Matthew Albert Hunter at Rensselaer Polytechnic Institute. Hunter achieved this by heating titanium tetrachloride ( $\text{TiCl}_4$ ) with sodium in a steel bomb. Finally in 1932, Wilhelm Justin Kroll discovered a way to produce larger amounts of titanium by combining  $\text{TiCl}_4$  with calcium. Later, he modified the reducing agent from calcium to magnesium, now called the Kroll Process. The Kroll process allowed for commercial production of titanium. After producing titanium tetrachloride from rutile or ilmenite, the reaction for producing pure titanium is as follows<sup>1</sup>:



Titanium is used primarily in the aerospace industry due to its high specific strength. Titanium's density ( $\sim 0.16\text{-}0.18 \text{ lb/in}^3$ ) is roughly half of steel's density ( $\sim 0.27\text{-}0.29 \text{ lb/in}^3$ ), but can be as strong as many carbon and stainless steels (Figure 1)<sup>2</sup>. Titanium has excellent corrosion resistance and is inert in the body, making it useful in the chemical and medical

industries. The automotive industry also makes limited use of titanium for engine components. Another attractive use for titanium is in high temperature applications, especially TiAl alloys. Specific strength of titanium alloys can compete with high temperature steels and Ni-base superalloys (Figure 2). Titanium at high temperature is limited by its oxidation behavior, but titanium aluminides help with this limitation<sup>1</sup>.

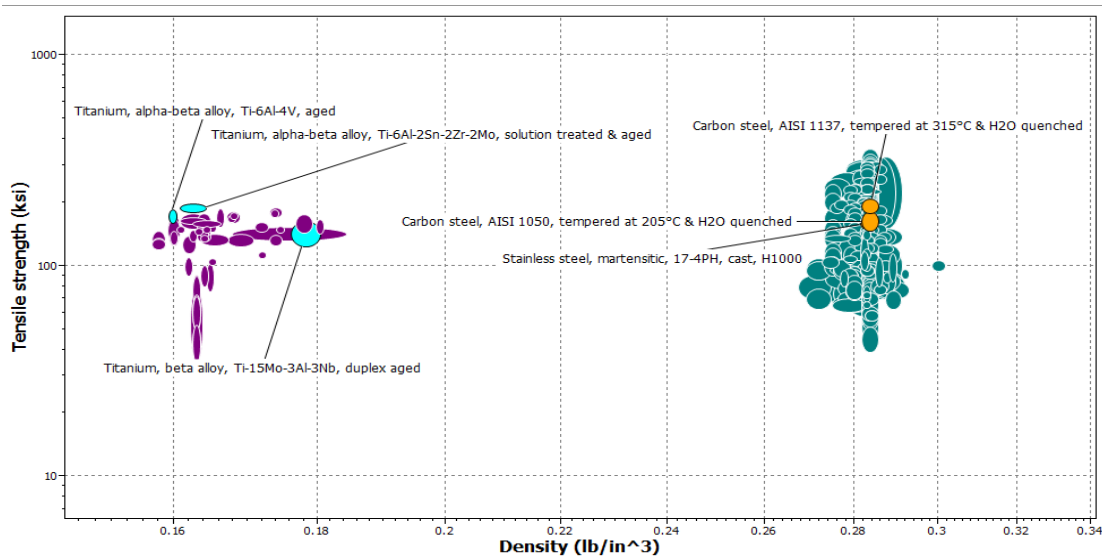


**Figure 1.** Tensile strength vs density for titanium and steel. Purple circles represent titanium alloys and teal represents steels. Light blue circles are specifically labeled titanium alloys and orange are specifically labeled steels<sup>2</sup>.

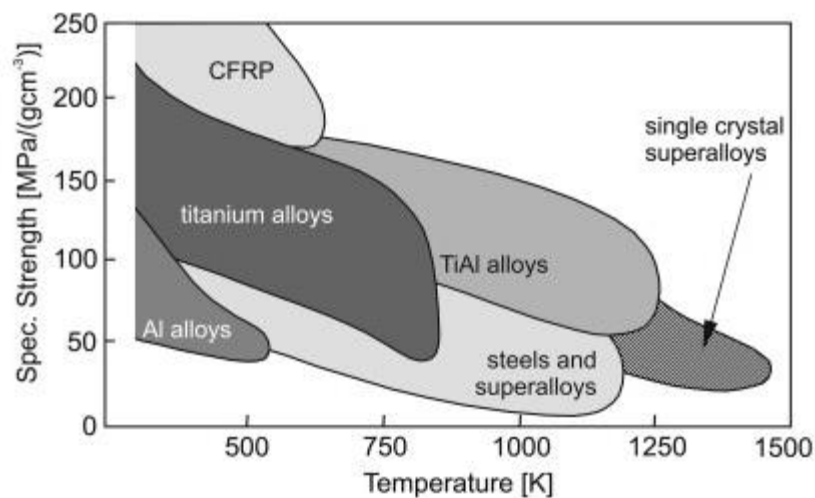


**Figure 2.** Specific strength vs temperature for titanium alloys and other structural materials<sup>1</sup>.



### A.3 Titanium Phases

Titanium has two main phases,  $\alpha$  and  $\beta$ . In pure titanium,  $\alpha$  is the low temperature stable phase and  $\beta$  the high temperature stable phase. A temperature called the  $\beta$ -transus is the point where  $\alpha$  transforms into  $\beta$  ( $\approx 1620^\circ\text{F}$ )<sup>1</sup>. Titanium also has two martensites,  $\alpha'$  and  $\alpha''$ .

#### A.3.1 Alpha Titanium

The low temperature  $\alpha$  phase has a hexagonal close packed (HCP) crystal structure (Figure 3a). The ideal  $c/a$  ratio for HCP is 1.633. Titanium has a ratio of 1.587, with lattice parameters of  $a=0.295\text{nm}$  and  $c=0.468\text{nm}$ <sup>1</sup>. Interstitial atoms such as carbon, nitrogen, or oxygen increase the  $c/a$  ratio. The non-ideal packing leads to slip favored on prism planes rather than on basal planes (Figure 3b)<sup>1</sup>.

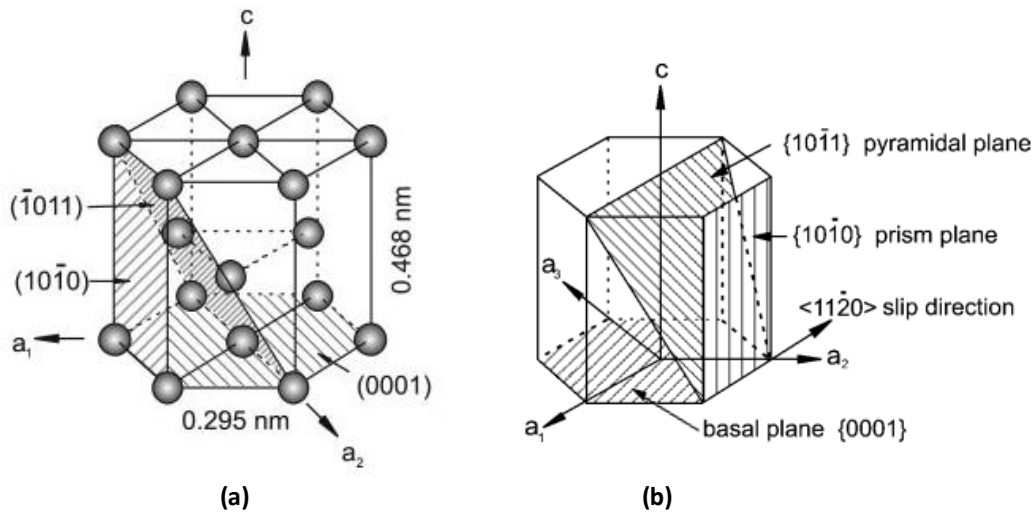


**Figure 3.** Hexagonal close packed structure of  $\alpha$ -Ti with a) showing the lattice parameters and b) the slip planes<sup>1</sup>.

The HCP nature of the  $\alpha$  phase gives limited plastic deformation due to HCP having only four of the five independent slip systems required for plastic deformation. So although the packing density of an HCP slip plane is 91%, deformation is harder than in BCC materials with a slip plane packing density of 83%<sup>1</sup>. But the crystal structure of  $\alpha$ -Ti results in good strength and creep resistance<sup>3</sup>. Single crystalline  $\alpha$ -Ti also exhibits clear anisotropy also due to being HCP. Young's modulus perpendicular to the basal plane is about 145GPa, while only 100GPa parallel to the basal plane<sup>1</sup>.

### A.3.2 Beta Titanium

Above the  $\beta$  transus in pure titanium,  $\alpha$ -Ti transforms into the body centered cubic (BCC) phase  $\beta$  (Figure 4). Ductility is greater in  $\beta$ -Ti due to BCC having more slip systems than HCP, as well as a shorter minimum slip path. HCP has a minimum slip path length of  $b_{\min} = 1a$ , while BCC's is  $b_{\min} = 0.87a^1$ . More slip systems and shorter minimum slip path length contribute to  $\beta$ -Ti's increased ductility over  $\alpha$ -Ti, even though BCC's packing density on slip planes is less.

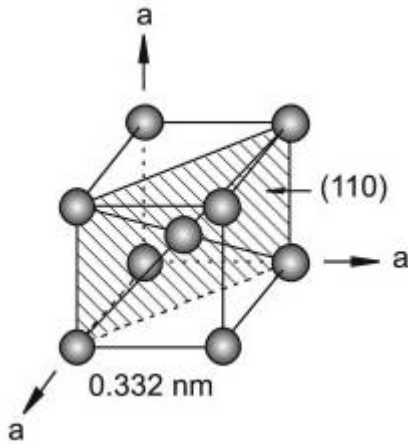


**Figure 5.** Body centered cubic structure of  $\beta$ -Ti<sup>1</sup>.

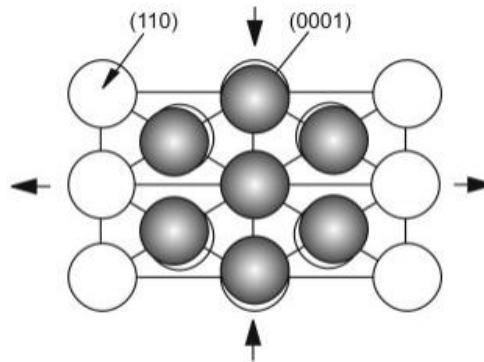


**Figure 4.** The  $\beta$  to  $\alpha$  transformation showing the (110) BCC planes in white and the (0001) HCP basal plane in gray<sup>1</sup>.

### A.3.4 Beta to Alpha Transformation

Cooling from the  $\beta$  phase field results in the most densely packed BCC planes  $\{110\}$  to become the basal planes  $\{0001\}$  of HCP  $\alpha$  (Figure 5)<sup>1</sup>. The distance between the HCP basal planes is slightly larger than the distance between BCC  $\{110\}$  planes, causing a contraction of the c-axis relative to the a-axis<sup>1</sup>. The slight change in distance distorts the HCP lattice, leading to the non-ideal c/a ratio as previously mentioned<sup>1</sup>. A slight increase in volume is also observed when cooling from  $\beta$ -Ti to  $\alpha$ -Ti<sup>1</sup>.

The  $\beta$  to  $\alpha$  transformation is thought to be a diffusionless martensitic transformation, and cannot be suppressed by rapid quenching without the addition of alloying elements<sup>3</sup>. Quenching at temperatures above the martensite start temperature,  $\beta$  transforms into a fine plate-like martensitic structure known as  $\alpha'$ . The  $\alpha'$  martensite has an HCP structure with a

similar orientation relationship as  $\beta$  to  $\alpha$ . The  $\alpha''$  martensite has an orthorhombic structure and is formed upon quenching from temperatures below about 1652°C<sup>1</sup>.

The BCC unit cell for  $\beta$ -Ti, with six slip planes and two slip directions, gives 12 potential orientations for  $\alpha$ -Ti<sup>1</sup>. The limited number of orientations for  $\alpha$ -Ti to form results in repeated orientations of  $\alpha$ -Ti packets. This leads to a lamellar basket-weave structure upon cooling below the  $\beta$ -transus (Figure 6)<sup>1</sup>. Slower cooling results in a coarser basket-weave structure, faster cooling a finer basket-weave structure.

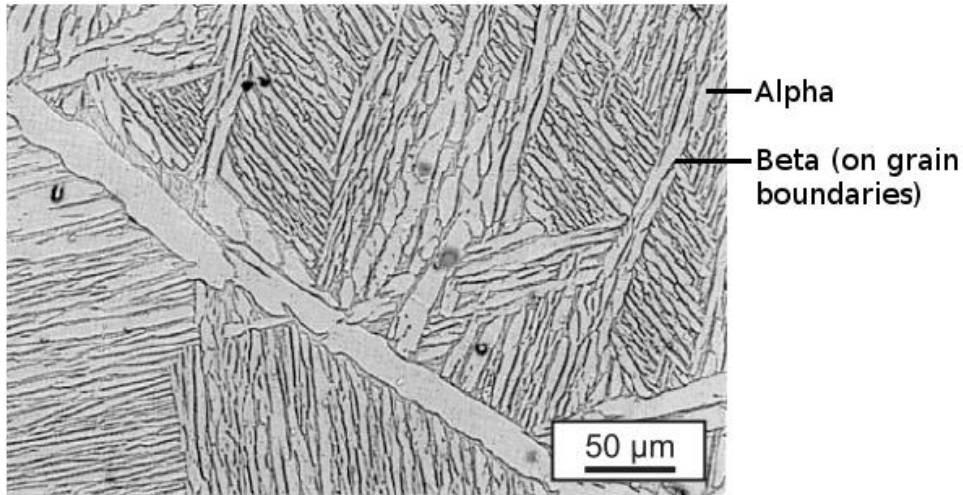


**Figure 6.** Lamellar basket-weave structure of  $\alpha$ -Ti in Ti-6Al-4V<sup>1</sup>. Alpha is the lighter color phase and beta is the darker color phase on the grain boundaries.

#### A.4 Classifying Titanium Alloys

Titanium alloys have three main classifications:  $\alpha$  alloys,  $\alpha + \beta$  alloys, and  $\beta$  alloys. The type of alloy depends on alloying elements, known as  $\alpha$  or  $\beta$  stabilizers (Figure 7)<sup>1</sup>.

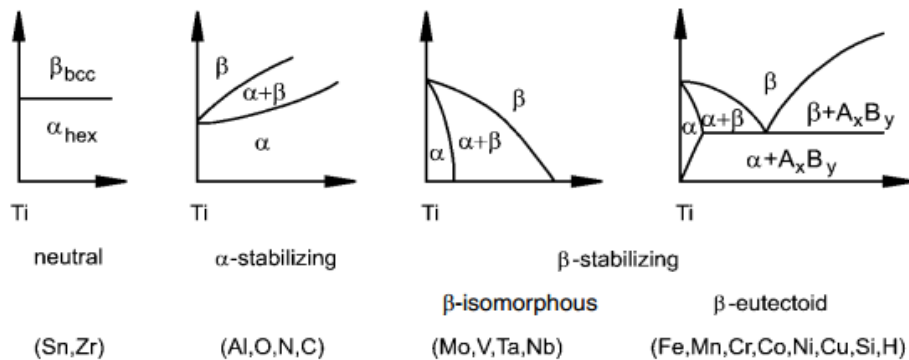


**Figure 7.** Schematic representation of the alloying element categories for titanium<sup>1</sup>.

Aluminum and the interstitial elements C, O, and N are the most important  $\alpha$  stabilizers<sup>1,3</sup>. Boron is also classified as an  $\alpha$  stabilizer, but has little effect on the  $\beta$ -transus due to low solid solubility (<0.02%)<sup>4</sup>. Boron has been reported to cause an apparent increase of the  $\beta$ -transus in Ti-6Al-4V due to the combined effect of supersaturation of boron during quenching in combination with the equilibrium boron in solution<sup>4</sup>. A two phase  $\alpha + \beta$  region is also formed by  $\alpha$  stabilizers in addition to extending the  $\alpha$  phase field to higher temperatures<sup>1</sup>.

The  $\beta$  stabilizing elements can be divided into two categories,  $\beta$ -isomorphous and  $\beta$ -eutectoid. Elements that fall under  $\beta$ -isomorphous have a higher solubility in  $\beta$ -Ti and do not form intermetallics<sup>1</sup>. The most important  $\beta$ -isomorphous elements are Mo, V, and Ta<sup>1</sup>.

The  $\beta$ -eutectoid elements form a eutectoid and intermetallics. The eutectoid reaction is  $\beta \rightarrow \alpha + A_xB_y$ . Intermetallics are formed due to lower solubility in  $\beta$ -Ti. Elements in the  $\beta$ -eutectoid category include Fe, Mn, Cr, Co, Ni, Cu, Si, and H<sup>1</sup>.

#### **A.4.1 Alpha Alloys**

The  $\alpha$  alloys often contain Al, Sn, or both. Al has a solid solution strengthening effect on titanium, but reduces ductility<sup>3</sup>. Sn is neutral in its effect on the phase diagram, but Sn strengthens titanium without a significant loss in ductility<sup>3</sup>. The  $\alpha$  alloys generally have good strength, toughness, creep resistance, and weldability. But these alloys cannot be strengthened by heat treating due to having only one phase and have poorer forgeability than other titanium alloys<sup>5</sup>.

Some  $\alpha$  alloys have extra low levels of interstitials (ELI), such as Ti-5Al-2.5Sn-ELI. These alloys retain ductility and toughness at cryogenic temperatures because of the lack of a ductile-brittle transformation like BCC alloys show. Therefore these  $\alpha$  alloys are used in cryogenic applications<sup>3</sup>. If  $\alpha$  alloys have small amounts of a  $\beta$  stabilizer added, they are referred to as near- $\alpha$  and will contain some retained  $\beta$ <sup>1,3</sup>.

#### A.4.2 Beta Alloys

The  $\beta$  alloys are also called metastable  $\beta$  alloys. They contain one or more  $\beta$  stabilizers like Mo, V, or Cr in sufficient quantity to suppress the martensitic transformation<sup>1</sup>. These alloys have high hardenability and forgeability<sup>3</sup>. But since  $\beta$  is BCC, it is susceptible to a ductile-brittle transformation and therefore  $\beta$  alloys are not suited for low temperature applications<sup>3</sup>.

Solution treated  $\beta$  alloys have good ductility, toughness, and cold formability<sup>3</sup>. Metastable  $\beta$  alloys can be age hardened to transform some of the metastable  $\beta$  to  $\alpha$ , and can still contain an  $\alpha$  fraction of 50% or more<sup>1,3</sup>. The disadvantages to  $\beta$  alloys compared to  $\alpha + \beta$  alloys are higher density, lower creep resistance, and lower tensile ductility in the aged condition<sup>5</sup>.

#### A.4.3 Alpha-Beta Alloys

Ti-6Al-4V is an  $\alpha + \beta$  alloy and the subject of this project; the  $\alpha + \beta$  alloys are the most widely used titanium alloys. They contain  $\alpha$  and  $\beta$  stabilizers so that the alloys have a mixture of  $\alpha$  and  $\beta$  at room temperature, with about 5-40%  $\beta$ <sup>1</sup>. These alloys can be strengthened by heat treatment. The heat treatment procedure involves heating to a solution-treating temperature, quenching, and then aging. At the solution-treating temperature primary  $\alpha$  and  $\beta$  are formed. Upon quenching from the solution-treating temperature metastable  $\beta$  may be retained, or the  $\beta$  may transform into  $\alpha$  by nucleation and growth or  $\alpha'$  martensite with some retained metastable  $\beta$ <sup>3,5</sup>. The specific response of  $\beta$  depends on the alloy composition (martensite start temperature), cooling rate, solution-treating temperature, and section size<sup>5</sup>. The aging step is done at 896-1202°F to precipitate  $\alpha$  and produce a fine mixture of coherent  $\alpha + \beta$  in the retained or transformed  $\beta$  phase (acicular  $\alpha$  or martensite)<sup>3,5</sup>.

For  $\alpha + \beta$  alloys heating to a temperature above the  $\beta$ -transus leads to uninhibited  $\beta$  grain growth due to the lack of  $\alpha$  grains. Subsequent age hardening would occur mostly at the  $\beta$  grain boundaries and have an inhomogeneous distribution<sup>3</sup>. This result reduces the ductility of the alloys<sup>3</sup>.

Solution-treating and aging can increase the strength of  $\alpha + \beta$  alloys by 30-50% or more from the annealed or over-aged condition<sup>5</sup>. Alloys relatively low in  $\beta$  stabilizers, like Ti-6Al-4V,

have poor hardenability and must be quenched rapidly to achieve significant strengthening<sup>5</sup>. Heat treatment response is also dependent on section size. Water quenching is not rapid enough for Ti-6Al-4V to significantly harden sections larger than about 1in, but other alloys (Ti-5Al-2Sn-2Zr-4Mo-4Cr) can be relatively uniformly hardened throughout sections up to 6in thick<sup>5</sup>.

Of the  $\alpha + \beta$  alloys, Ti-6Al-4V is the most widely used. It has an excellent combination of strength, toughness, and corrosion resistance<sup>5</sup>. Since this project involves Ti-6Al-4V, the remainder of this report will address Ti-6Al-4V specifically.

### **A.5 Ti-6Al-4V Microstructure**

Slowly cooling from the  $\beta$  region in Ti-6Al-4V results in  $\alpha$  plates forming. As previously mentioned, the HCP basal planes of  $\alpha$  {0001} form parallel to the BCC {110} planes of  $\beta$ . The  $\alpha$  phase grows quickly parallel to the {110} BCC planes, but slowly perpendicular to these planes<sup>5</sup>. A Widmanstätten microstructure is formed with  $\alpha$  plates separated by retained  $\beta$  phase<sup>5</sup>. Widmanstätten structures are formed when one phase transforms with a crystallographic relationship to the phase it transformed from<sup>3,5</sup>. Figure 8(i) shows the slow cooled microstructure from the  $\beta$  region.

Upon rapid cooling from the single phase  $\beta$  region,  $\beta$  will decompose into either  $\alpha'$  or  $\alpha''$  martensite depending on composition and quenching temperature<sup>5</sup>. Some retained  $\beta$  will likely remain due to the martensite finish temperature ( $M_f$ ) being below room temperature<sup>5</sup>. The quenched microstructure in this case is seen in Figure 8(a).

Of importance for this project is quenching from near the  $\beta$ -transus temperature in the  $\alpha + \beta$  region. Quenching from this region will result in primary  $\alpha$ ,  $\beta$ , and  $\alpha'$  martensite formed from high temperature  $\beta$ <sup>5,6</sup>. Primary  $\alpha$  is untransformed  $\alpha$  from the starting microstructure, also known as globular  $\alpha$ . Slower cooling will result in primary  $\alpha$  with secondary  $\alpha$ <sup>5,6</sup>. Like the martensites, secondary  $\alpha$  is formed from the high temperature  $\beta$ . Some  $\beta$  may also be present depending on composition. Figure 8(b) shows the quenched microstructure from the  $\alpha + \beta$  region.



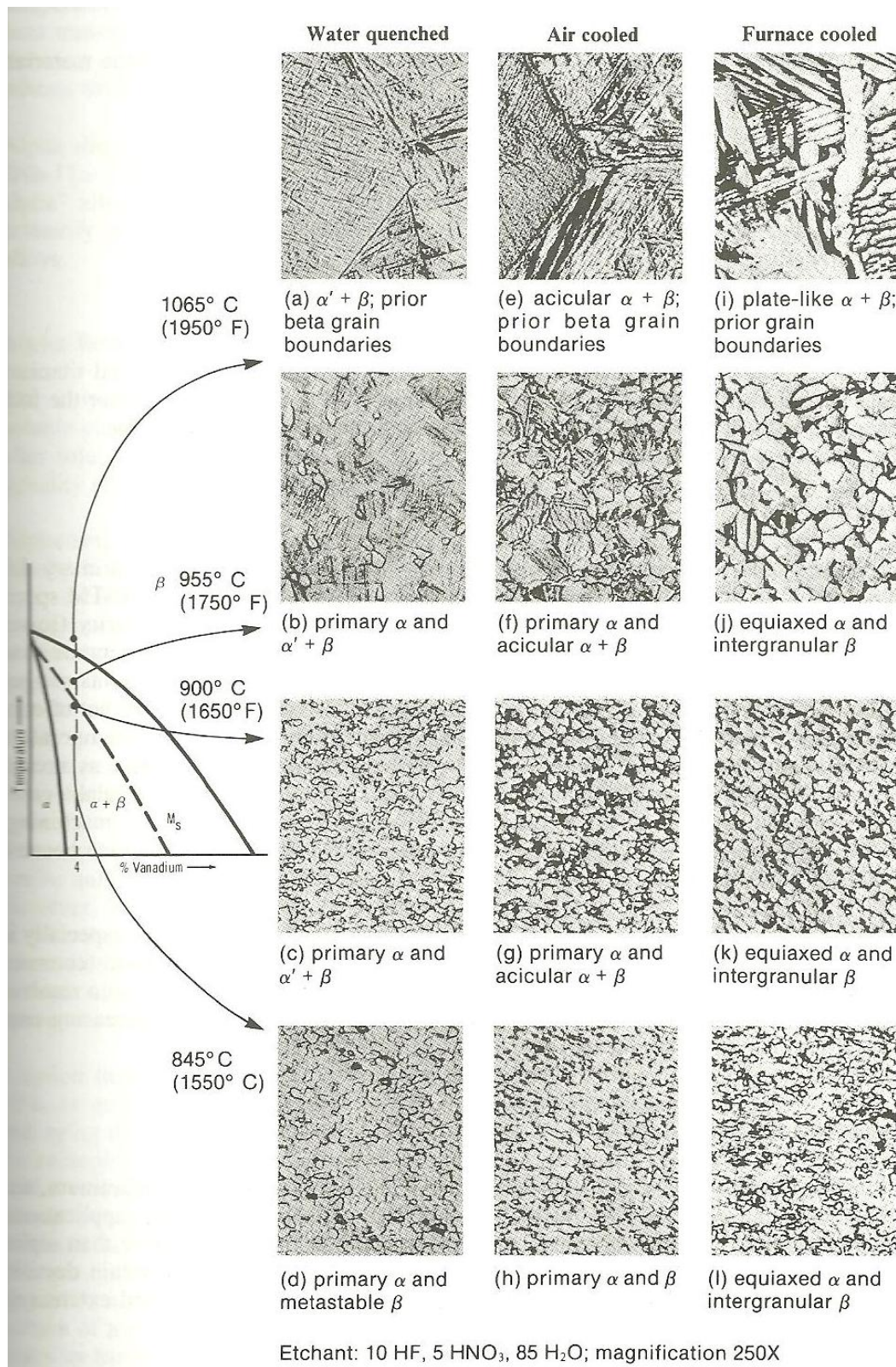


**Figure 8.** Microstructures of Ti-6Al-4V under three cooling rates and at four temperatures<sup>5</sup>. For this project (b) is the expected microstructure when quenching from below and  $\beta$ -transus, and (a) is the expected microstructure when quenching from above the  $\beta$ -transus.

## **A.6 Titanium Forging**

Titanium properties are greatly influenced by processing, so care must be taken to control the processing conditions. This influence of processing allows titanium to be tailored for a wide variety of applications with a minimum number of grades or alloys<sup>5</sup>. The wrought processing of  $\alpha + \beta$  titanium alloys often involves a series of hot working steps and final heat treatments<sup>7</sup>.

### **A.6.1 Primary Working**

Primary hot working's purpose is to produce a uniform and fine two-phase microstructure of globular  $\alpha$  in a matrix of  $\alpha$  and  $\beta$  from cast ingots<sup>7</sup>. This is accomplished by initial hot working and heat treatment in the single-phase  $\beta$  region followed by conversion of the lamellar structure into equiaxed  $\alpha + \beta$  by deformation below the beta transus<sup>1,7,8</sup>.

### **A.6.2 Die Forging**

Forging is a common wrought processing method for manufacturing titanium products and is typically conducted in the  $\alpha + \beta$  region. Forging sequences and heat treatment can be used to control the microstructure and resulting properties<sup>5</sup>. Knowledge of the  $\beta$ -transus is necessary for successful forging and heat treatment; the closer forging is conducted to the  $\beta$ -transus, the more  $\beta$  available to transform on cooling<sup>5</sup>. The exact form of the globular  $\alpha$  and transformed  $\beta$  structures produced by processing depends on the  $\beta$ -transus temperature<sup>5</sup>.

## **A.7 Broader Impacts**

Competition for the forging industry comes from investment casting, powder metallurgy processes, and machining from plates/slabs<sup>9</sup>. The main advantages for forging are the production of high quality, reliable, and longer life-cycle parts<sup>9</sup>. But forging does have some disadvantages like high acquisition cost, long lead time, and poorer metal utilization than other processes<sup>9</sup>. This project hopes to aid in forging manufacturability by preventing scrapped parts due to incomplete knowledge of the percent  $\alpha$  at high temperature during forging.

Six Sigma was successfully applied to copper forgings in China to increase copper utilization and decrease cost<sup>10</sup>. The cost savings was approximately \$250,000 per month after



identification of defect causes and implementation of solutions<sup>10</sup>. This project hopes to increase titanium utilization by reducing scrapped parts, resulting in lower costs and higher profits.

## B. Experimental Procedure

### B.1 Titanium Alloys

Weber Metals supplied seven different heats of Ti-6Al-4V ranging from lean to rich in carbon (Table I). The effect of carbon is the focus of this project, but nitrogen content is another potential variable. To limit the possible effect of nitrogen, heats similar as possible in nitrogen contents were chosen, but different in carbon for the first three compositions.

**Table I.** Ti-6Al-4V heats supplied and their carbon and nitrogen contents. Highlighted in yellow are the alloys tested

Heat (Sample Number)	Carbon (%)	Nitrogen (%)
9G25836 (1)	0.023	0.016
H15690 (2)	0.020	0.008
K37M (3)	0.032	0.004
K49M (4)	0.012	0.002
65EJ (5)	0.022	0.007
K39H (6)	0.014	0.003
81EC (7)	0.038	0.008

Initially, samples 4, 5, and 7 were chosen as low, medium, and high carbon contents, respectively. But due to an error in processing sample 5 was ruined and so replaced by sample 2 as the low carbon sample.

### B.2 Sample Preparation

Cubes were cut from forged converted (primary worked) ingot slices from the mid-radius to avoid any chemical segregation that may occur on the outside and inside of the ingot (Figure 9). Cubes were approximately 0.5in on each side.

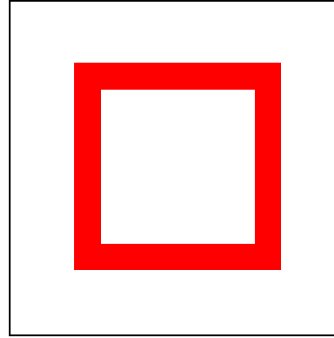
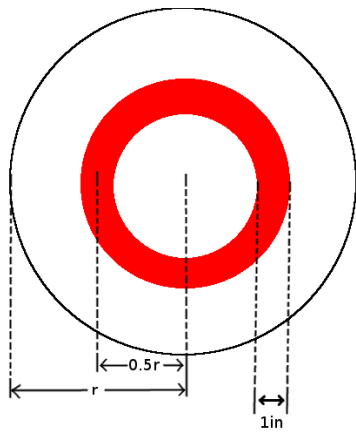


**Figure 9.** Diagram of locations on each converted ingot slice where cubes were cut. Both round (left) and square (right) slices were received.

### B.3 Testing Methodology

A high temperature furnace was used to heat treat each sample. A type K independent thermocouple was used for accuracy with a separate readout (Figure 10). To avoid temperature variations based on location within the furnace, high temperature bricks were used to raise the samples close to the three thermocouples inside the furnace (Figure 11).



**Figure 10.** High temperature furnace and separate temperature readout used for heat treating.

Since quench delay needed to be minimized to lock in the at-temperature microstructure, each cube was wrapped in steel wire with a loop to hook with tongs so that each sample could be quickly pulled from the furnace into a water quench. One high temperature brick was cut at an angle to facilitate easier and faster quenching (Figure 11). Thin wire wrapped around each cube and run out of the furnace to pull the cube into water was considered. But thin wire damaged the insulation between the door and furnace upon closing the door. The loop method was chosen to avoid any furnace damage. Quench delay using the loop method was three seconds or less.

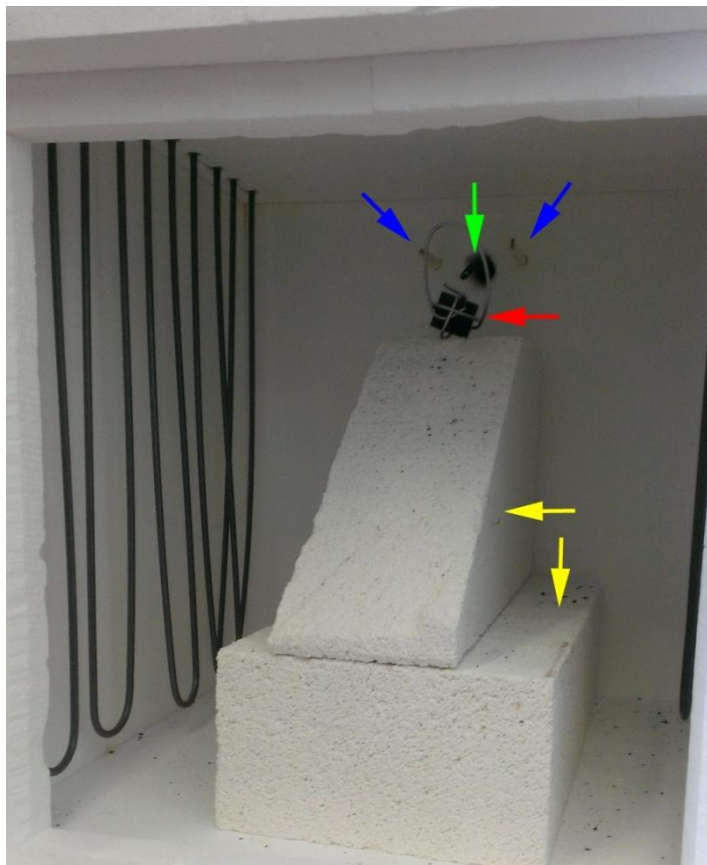


**Figure 11.** Setup inside the furnace: blue arrows point to the furnace thermocouples, the green arrow points to the independent thermocouple, the red arrow points to the sample wrapped in steel wire, and the yellow arrows point to high temperature bricks.

Cubes were held at their respective temperatures for 20 minutes to form the equilibrant of primary  $\alpha$ , before water quenching. After high temperature heat treating, cubes underwent an aging treatment at  $896 \pm 20^\circ\text{F}$  for one hour then were water quenched. The furnace only displayed Celsius, so cubes were heat treated in  $10^\circ\text{C}$  ( $18^\circ\text{F}$ ) increments. Metallography was conducted on each heat treated cube.

ASTM E562-11, Standard Test Method for Determining Volume Fraction by Systematic Manual Point Count, was utilized to find the volume fraction of  $\alpha$ . Following this standard, a grid of small dots was drawn on a transparency then placed on a computer screen connected to a camera on the microscope. Depending on microstructural clarity, fields were examined at 200x or 500x. Whenever a dot lay within a primary  $\alpha$  particle, 1 point was counted; whenever a dot lay on a primary  $\alpha$  grain boundary,  $\frac{1}{2}$  point was counted; whenever doubtful about the point being within or on a primary  $\alpha$  grain boundary,  $\frac{1}{2}$  point was counted<sup>11</sup>. To increase accuracy and decrease the amount of fields needing to be examined, a 100 point grid was used as recommended by the standard (Figure 12). A 100 point grid also allows for easier mathematical analysis since 1 point is 1% and  $\frac{1}{2}$  point is 0.5%. Five to twenty fields per sample are needed for analysis with a 100 point grid to achieve 10-20% relative accuracy, so twelve fields were counted per sample<sup>11</sup>.



**Figure 12.** Micrograph of a sample heat treated at 1735°F, quenched, then aged at 896°F. Overlaid is a 100 point grid representative of the grid used to point count. Circled in yellow is a primary  $\alpha$  particle.

## B.4 Realistic Constraints

Titanium's sensitivity to alloying elements makes microstructural prediction difficult based on the phase diagram alone; carbon is one of the important alloying elements on titanium's phase diagram. Knowing the effect of carbon will help with manufacturability by giving a closer estimate of the primary  $\alpha$  percentage based on carbon content.

Currently, the effect of carbon on primary alpha percent is unknown, leading to less accurate forging and higher potential for scrap. The ability to more accurately forge to specifications will produce less rejected parts, which increases profit and decreases loss due to scrap.

## C. Results

Average, standard deviation, 95% confidence interval, and percent relative accuracy were calculated for heat treatment for each allow. The ASTM standard provided equations for the 95% confidence interval (95%CI) and relative accuracy (%RA) (Equations 1, 2).

$$95\% CI = t \frac{s}{n} \quad (1)$$

Where  $t$  is 2.201, a confidence interval multiplier given in the ASTM standard for 12 analyzed fields per sample;  $s$  is the standard deviation; and  $n$  is the number of fields analyzed per sample.

$$\%RA = \frac{95\%CI}{P_p} 100 \quad (2)$$

Where  $P_p$  is the average of the 12 fields analyzed per sample.

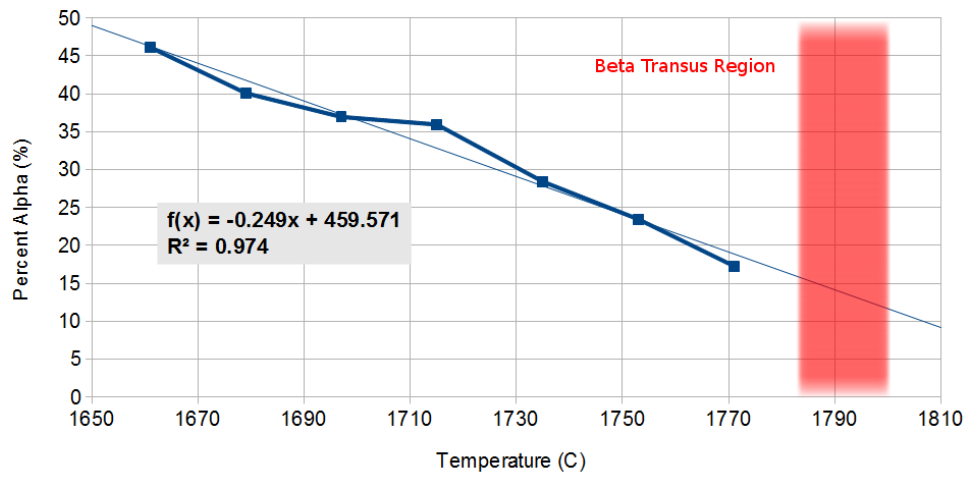
Averages of the 12 fields per sample were used as a comparison; the range of data overlapped between the different temperatures due to chemical segregation or error in the point counting. Each composition has one sample heated above the  $\beta$  transus, but this temperature does not necessarily represent the actual  $\beta$  transus temperature. Most samples had a 95%CI of less than 4% primary  $\alpha$ , with standard deviations larger than the 95%CI. The %RA ranged from 4-27%; it should also be noted that lower %RA is better (Table II).

**Table II.** Carbon content, heat treatment temperatures, average primary  $\alpha$ , and statistical data for each Ti-6Al-4V alloy.

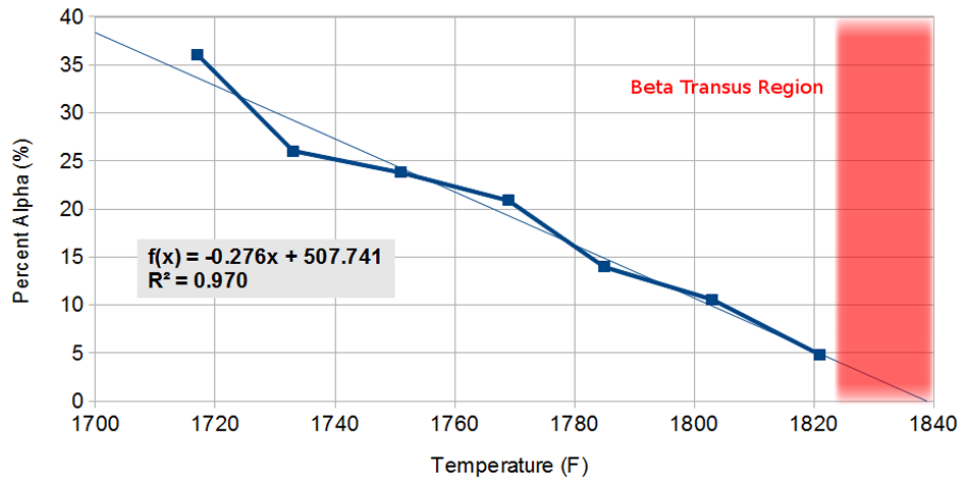
Composition (%C)	Temperature (°F)	Average Primary α (%α)	Standard Deviation (%α)	95% CI (%α)	Relative Accuracy (%)
0.012	1661	46	2.87	1.82	4.0
	1679	40	5.07	3.22	8.0
	1697	37	4.42	2.81	7.6
	1715	36	3.32	2.11	5.9
	1735	28	4.76	3.02	10.6
	1753	24	5.38	3.42	14.6
	1771	17	4.23	2.69	15.6
	1800 (above β transus)				
0.020	1717	36	5.14	3.26	9.0
	1733	26	4.56	2.90	11.1
	1751	24	5.94	3.78	15.9
	1769	21	3.57	2.27	10.9
	1785	14	3.58	2.27	16.3
	1803	11	3.03	1.92	18.2
	1821	5	2.10	1.34	27.7
	1841 (above β transus)				
0.038	1740	34	5.08	3.23	9.4
	1760	28	7.29	4.63	16.4
	1774	17	3.49	2.22	13.0
	1792	9	2.58	1.64	17.6
	1810	10	3.67	2.33	23.8
	1826 (above β transus)				

Plots of primary  $\alpha$  percent vs temperature were created for each composition. A plot of the 0.012%C Ti-6Al-4V alloy average primary  $\alpha$  percent displayed a linear trend with  $R^2=0.97$ . Only one point seemed to deviate from the trend, which is the one sample that had a longer quench delay than the other samples (Figure 13a). Plotting the average primary  $\alpha$  percent for 0.020%C alloy also displayed a linear trend, with a similar slope to the 0.012%C plot (Figure 13b). The trend appears to be shifted lower by 5-10% primary  $\alpha$  when compared with 0.012%C alloy. Although the low and medium carbon compositions showed a linear trend, the high carbon 0.038%C alloy did not show the same linearity (Figure 13c), but still had an  $R^2=0.91$  with a linear regression fit. The linear regression fit slopes were -0.249, -0.276, and -0.392 for the low, medium, and high carbon alloys respectively.

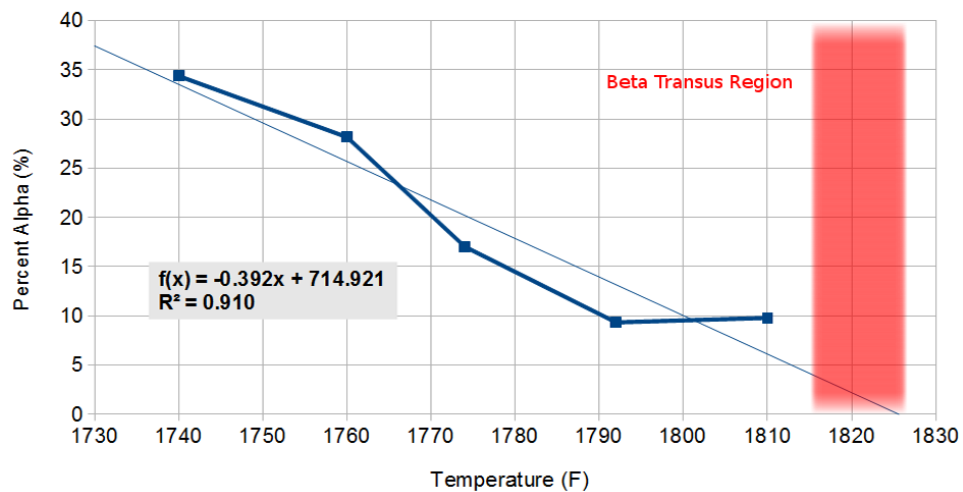




(a)



(b)



(c)

**Figure 13.** Plots of average primary alpha percent for (a) the 0.012%C alloy, (b) the 0.020%C alloy, and (c) the 0.038%C alloy. Also shown are linear regression equations for each plot. The low and medium carbon alloys showed the most linearity.

Boxplots of the testing data show a wide range of observed primary  $\alpha$  percentages with variations up to 30% within a single sample, although most had 10-15% variation. On the boxplots the black dot is the mean, the box is the middle two quartiles of data, the horizontal line is the median, and an asterisk is an outlier (Figure 14).

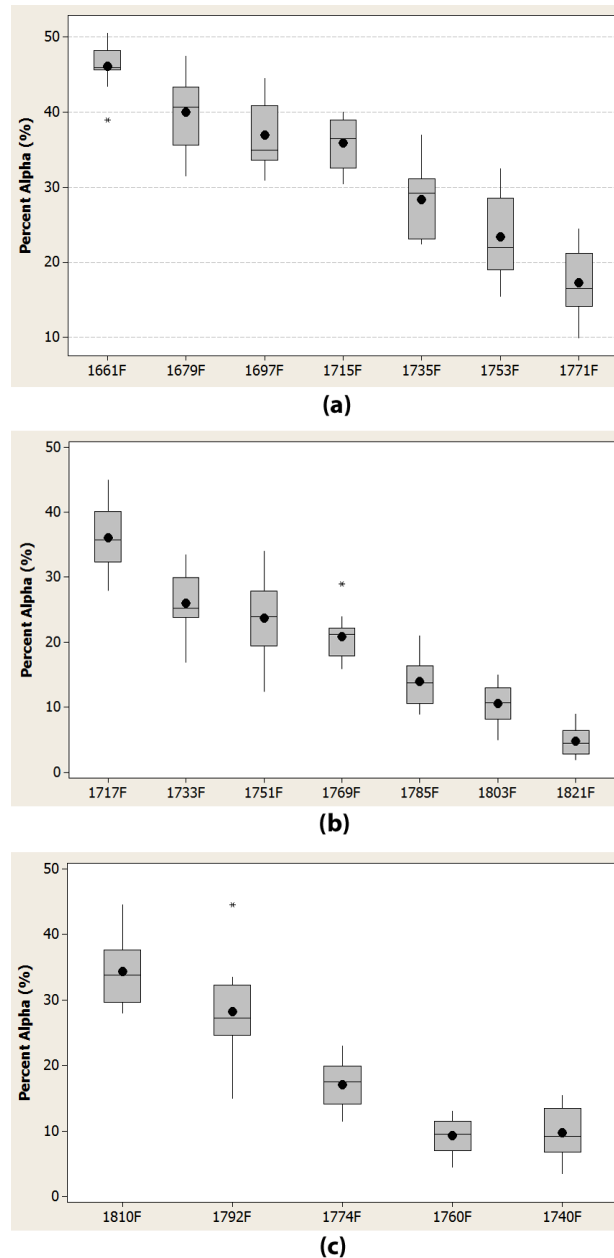


**Figure 14.** Boxplots for (a) the 0.012%C alloy, (b) the 0.020%C alloy, and (c) the 0.038%C alloy. The black dot represents the mean, the box represents the middle two quartiles of data, and the line through the box is the median. Outliers are shown by asterisks. The range was as large as 30% primary alpha for each sample, although most had a range of about 15% primary alpha.

## D. Discussion

The curves for the 0.012%C and 0.020%C alloys showed linearity with  $R^2=0.97$  for each. This is not unreasonable when looking at the phase diagram for Ti-6Al-4V, which appears fairly linear between the  $\beta$  transus and  $\beta$  minus 100°F (Figure 19). The 0.038%C sample deviated from the linearity of the low and medium carbon samples, but still had an  $R^2=0.91$  with a linear regression. The regression equation for 0.038%C may be a good approximation, but should not be taken as proof of linearity.

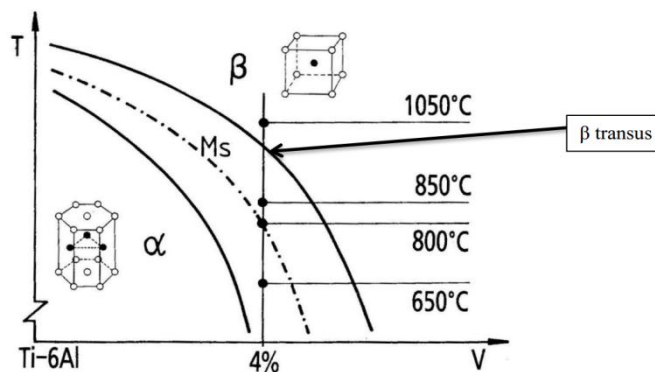


**Figure 15.** Representative phase diagram for Ti-6Al-4V. Temperatures are only approximate.

The effect of carbon on rate of primary  $\alpha$  decrease was the same between the low and medium carbon alloys. But the medium carbon alloy averages and trend line appear to be shifted lower by 5-10% primary  $\alpha$  when measuring percentage at temperatures relative to the  $\beta$  transus. The 0.038%C sample also appears to be shifted down 5-10% primary  $\alpha$  when compared to the 0.012%C sample.

It is possible that overestimation on the first round of testing occurred for low carbon alloy since the point counting process was still being learned. But it is also possible that higher carbon content does shift the primary  $\alpha$  percent down 5-10%. Assuming no error in point counting or heat treating for low carbon alloy, it appears the linear trend deviates as temperature gets within 20-30°F of the  $\beta$  transus.

The medium carbon alloy had the highest sample heated above the  $\beta$  transus of 1841°F compared to 1800°F and 1826°F for the low (0.012%C) and high (0.038%C) carbon alloys. The  $\beta$  transus could fall within the temperature range between the samples that straddle the  $\beta$  transus, but even so the medium carbon alloy appears to have a similar  $\beta$  transus to the high carbon alloy. Other than carbon content, both the medium and high carbon alloys had similar oxygen and nitrogen contents. Oxygen and nitrogen are other potential factors on the  $\beta$  transus temperature and/or primary  $\alpha$  percentage, but it is doubtful they had much effect considering similarity in content for each alloy.

## E. Conclusions

1. Low and medium carbon samples decrease in primary  $\alpha$  linearly with temperature, with slopes of -0.249 and -0.276, respectively.
2. Carbon does not appear to affect the slope of primary  $\alpha$  percent decrease when comparing 0.012%C and 0.020%C Ti-6Al-4V alloys.
3. Carbon may have an effect at higher amounts, seen by the deviation in linearity of the 0.038%C alloy and the steeper slope of -0.392 as compared to the low and medium carbon slopes.
4. The medium and high carbon alloys are shifted lower by 5-10% primary  $\alpha$  compared to the low carbon alloy. It is unclear whether this is due to carbon effect, error in heat treatment, or error in point counting.

## F. References

1. Leyens, Christoph, and Manfred Peters. *Titanium and Titanium Alloys*. Weinheim, Germany: Wiley-VCH, 2003. Print.
2. Granta CES 2012 (Version 11.9.9). Granta Design Limited. Cambridge, United Kingdom.
3. Abbaschian, Reza, Lara Abbaschian, and Robert E. Reed-Hill. *Physical Metallurgy Principles*. 4th Ed. Stamford, CT: Cengage Learning, 2009. Print.
4. Tamirisakandala, S., R.B. Bhat, D.B. Miracle, S. Boddapati, R. Bordia, R. Vanover, and V.K. Vasudevan. "Effect of boron on the beta transus of Ti-6Al-4V alloy." *Scripta Materialia* 53 (2005): 217-222. Print.
5. Donachie Jr., Matthew J. *Titanium: A Technical Guide*. Metals Park, Ohio: ASM International, 1988. Print.
6. Ding, R., Z.X. Guo, and A. Wilson. "Microstructural evolution of a Ti-6Al-4V alloy during thermomechanical processing." *Materials Science and Engineering A327* (2002): 233-245. Print.
7. Semiatin, S.L., S.L. Kinsley, P.N. Fagin, F. Zhang, and D.R. Barker. "Microstructural Evolution during Alpha-Beta Heat Treatment of Ti-6Al-4V." *Metallurgical and Materials Transactions* 34A (2003): 2377-2386. Print.
8. Seshacharyulu, T., S.C. Medeiros, W.G. Frazier, and Y.V.R.K. Prasad. "Hot working of commercial Ti-6Al-4V with an equiaxed  $\alpha$ - $\beta$  microstructure: materials modeling considerations." *Materials Science and Engineering A284* (2000): 184-194. Print.
9. Barnett, Kerry J. "Research initiatives for the forging industry." *Journal of Materials Processing Technology* 98 (2000): 162-164. Print.
10. Liu, J. "Application of Six Sigma methodology in forging manufacturing plants: an example study." *Computing Control and Industrial Engineering* 2 (2011): 354-357. Print.
11. ASTM Standard E562, 2011, "Standard Test Method for Determining Volume Fraction by Systematic Manual Point Count," ASTM International, West Conshohocken, PA, 2011, DOI: 10.1520/E0562-11.

